

Generation of spin squeezing via a fully quantum degenerate parametric amplifier

Yang Liu,^{1,2} Jie Song,³ Wei Qin,^{4,*} Ye-Hong Chen,^{4,5,1,2,†} and Yan Xia^{1,2,‡}

¹Fujian Key Laboratory of Quantum Information and Quantum Optics, Fuzhou University, Fuzhou 350108, China

²Department of Physics, Fuzhou University, Fuzhou 350108, China

³School of Physics, Harbin Institute of Technology, Harbin 150001, China

⁴Theoretical Quantum Physics Laboratory, RIKEN Cluster for Pioneering Research, Wako-shi, Saitama 351-0198, Japan

⁵Quantum Information Physics Theory Research Team,

RIKEN Center for Quantum computing (RQC), Wako-shi, Saitama 351-0198, Japan

Spin squeezing is one of the most attractive methods for realizing high-precision metrology. In this paper, we propose a protocol for generating spin squeezing in an atomic ensemble via a fully quantum degenerate parametric amplifier. We discuss the properties of generating spin squeezing with and without driving the pump cavity. Numerical simulation results show that the generated spin squeezing strength is sizable, and is able to be comparable to that obtained using a two-axis twisting (TAT) model. Moreover, we demonstrate that the protocol is experimentally feasible by introducing the corresponding experimental parameters. Therefore, the proposed protocol provides a promising approach to realize spin squeezing in photon-spin coupling systems.

I. INTRODUCTION

Spin squeezing, which reduces the fluctuation noise of one quadrature in phase space but increases the fluctuation noise of the other quadrature, has shown its advantages in quantum metrology [1–4]. Up to now, spin squeezing has been applied in many fields requiring high-precision measurements, such as Ramsey spectroscopy [5–8], atomic clocks [9–11], and gravitational-wave interferometers [12, 13]. Due to these promising applications, significant efforts have been devoted to generating spin squeezing in many physical systems, such as molecules [14, 15] and atomic ensembles [16–33]. Among the proposed protocols for atomic ensembles, the basic methods rely upon, e.g., quantum nondemolition measurement (QNDM) [23, 24], and nonlinear one-axis twisting (OAT) [25, 26] or two-axis twisting (TAT) [31–33] spin-spin coupling. It has been shown that different methods have different suppression effects on quantum fluctuations. For an ensemble with N atoms, the maximum amounts of squeezing, obtained with QNDM, OAT, and TAT, scale as $N^{-1/2}$, $N^{-2/3}$, and N^{-1} (the ideal Heisenberg limit), respectively [1].

Due to the ability to reduce the quantum fluctuation noise to the fundamental Heisenberg limit, TAT squeezing is considered as superior to other methods. Thus in the past few decades, many protocols [30–33] have been proposed to generate spin squeezing by constructing the TAT interaction. These protocols include, e.g., exploiting the Raman processes in the the Bose-Einstein condensates (BEC) [30], transforming from the OAT interaction [31], coupling the spin ensembles with a parametric driven cavity [32], and modifying a phase-locked atom-photon coupling [33]. However, there are

always some difficulties in applying these theoretical protocols to experimental implementations. Indeed, these difficulties include, e.g., the imperfect cooling [30], the imprecise time control [31], the introduced squeezing noise [32], and the complex pump drivings [33]. Recently, Macri *et al.* [27] proposed an interesting protocol for generating spin squeezing via an effective cavity-induced TAT-like interaction constructed by one-photon-two-atom excitation processes. This protocol paves a promising way to construct the TAT model and seems to be able to generate significant amount of squeezing. However, this protocol relies on a specific atom-cavity coupling (e.g., a transverse coupling), which cannot be collectively enhanced in atomic ensembles. This makes the strength of one-photon-two-atom processes extremely weak in typical ensemble-cavity systems.

To address the problem, we propose a protocol for generating spin squeezing in atomic ensembles by using a fully quantum degenerate parametric amplifier (DPA) [34]. Here, the DPA is represented by two parametrically coupled single-mode cavities, i.e., a pump cavity and a signal cavity. An effective Hamiltonian describing the cavity-induced TAT-like interaction is obtained through tuning the system parameters. The strength of the generated spin squeezing is determined by the properties of the pump cavity, such as the initial state, driving strength, and cavity decay. Specifically, we study the generation of spin squeezing with and without driving the pump cavity mode. Numerical simulations show that with and without driving the pump cavity mode, a sizable spin squeezing can be generated. In particular, for a strong driving strength and a strong pump cavity decay, the resulting spin squeezing strength is comparable with that of the TAT squeezing. Meanwhile, we investigate the sensitivity of the generated spin squeezing to the decoherence, including the decay of the cavities, the spontaneous emission of the atoms, and the collective dephasing of the atomic ensemble. The results show that the protocol is robust to the spontaneous emission of the atoms and the decay of the signal cavity. Additionally,

* wei.qin@riken.jp

† yehong.chen@riken.jp

‡ xia-208@163.com

the experimental feasibility of the protocol is also discussed by using current experimental parameters [35–46].

The rest part of the paper is organized as follows. In Sec. II, we give a brief description about the physical model and derive its effective Hamiltonian. In Sec. III, we study the generation of spin squeezing in an atomic ensemble. In Sec. IV, we show the experimental feasibility of the protocol. The conclusion of the present paper is summarised in Sec. V.

II. PHYSICAL MODEL AND EFFECTIVE DYNAMICS

In this paper, as shown in Fig. 1, we consider a system consisting of two parametrically coupled single-mode cavities (a pump cavity and a signal cavity), and an ensemble of N identical two-level atoms placed in the signal cavity. The resonance frequencies of the pump cavity and the signal cavity are assumed to be ω_p and ω_s , respectively. The parametric coupling of strength J describes a nonlinear conversion between a single pump photon and a pair of signal photons. Note that the strength J , which ranges from some tens of kHz to some tens of MHz, has been realized in recent experimental advances [35–38]. Therefore, the pump cavity and the signal cavity constitute a fully quantum degenerate parametric amplifier (DPA). We apply a classical driving field of frequency ω_l and amplitude Ω to the pump cavity. Meanwhile, the atoms of transition frequency ω_q couple to the signal cavity with a strength g . The Hamiltonian of the system can accordingly be written as (in the units of \hbar) [47]

$$\begin{aligned} \hat{H}_{\text{sys}} = & \omega_s \hat{a}_s^\dagger \hat{a}_s + \omega_p \hat{a}_p^\dagger \hat{a}_p + \omega_q \hat{S}_z + g(\hat{a}_s \hat{S}_+ + \hat{a}_s^\dagger \hat{S}_-) \\ & + \left(\frac{\Omega^*}{2} \hat{a}_p e^{i\omega_l t} + \frac{\Omega}{2} \hat{a}_p^\dagger e^{-i\omega_l t} \right) + J(\hat{a}_p \hat{a}_s^{\dagger 2} + \hat{a}_p^\dagger \hat{a}_s^2), \end{aligned} \quad (1)$$

where \hat{a}_s^\dagger (\hat{a}_p^\dagger) and \hat{a}_s (\hat{a}_p) are the creation operator and the annihilation operator of the signal (pump) cavity, respectively. Moreover, $\hat{S}_u = \sum_k \hat{\sigma}_k^u / 2$ ($k = 1, 2, \dots, N$) is the collective spin operator and $\hat{\sigma}_k^u$ ($u = x, y, z$) is the Pauli operator of the k th atom. $\hat{S}_+ = \hat{S}_x + i\hat{S}_y$ and $\hat{S}_- = \hat{S}_x - i\hat{S}_y$ are the raising and lowering operators of the collective spin, respectively. For simplicity, we set hereafter $g_c = \sqrt{N}g$ as the strength of the collective coupling between the ensemble and the cavity, and further assume that $\omega_p \simeq \omega_l \simeq 2\omega_q \simeq 2\omega_s$. In the rotation frame of reference of $\hat{H}_0 = \omega_l(\hat{a}_s^\dagger \hat{a}_s + 2\hat{a}_p^\dagger \hat{a}_p + \hat{S}_z)$, when $\omega_l \gg \{g_c, J\}$, one can obtain

$$\begin{aligned} \hat{H}_I = & \delta_p \hat{a}_p^\dagger \hat{a}_p + \delta_s \hat{a}_s^\dagger \hat{a}_s + \delta_q \hat{S}_z \\ & + (J \hat{a}_p \hat{a}_s^{\dagger 2} + g \hat{a}_s \hat{S}_+ + \frac{\Omega^*}{2} \hat{a}_p + \text{H.c.}), \end{aligned} \quad (2)$$

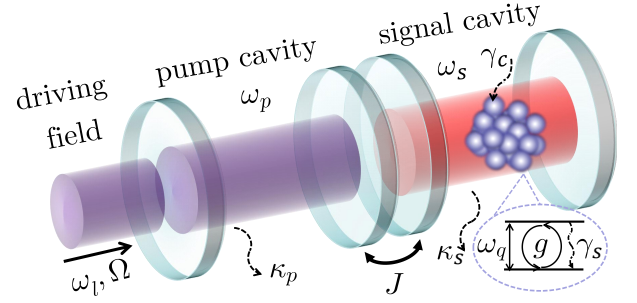


FIG. 1. Physical model of the protocol. Two single-mode cavities, the pump cavity and the signal cavity, are coupled with a parametric coupling of strength J . An ensemble of N identical two-level atoms is located inside the signal cavity, and is coupled to this cavity with a single-photon single-atom coupling strength g . ω_p (ω_s) is the resonance frequency of the pump (signal) cavity. A driving field of frequency ω_l and amplitude Ω is applied to the pump cavity. ω_q is the transition frequency of atoms, κ_p (κ_s) is the single-photon dissipation rate of the pump (signal) cavity, γ_s is the spontaneous emission rate of atoms, and γ_c represents the collective dephasing of the atomic ensemble.

where $\delta_q = \omega_q - \omega_l$, $\delta_s = \omega_s - \omega_l$, and $\delta_p = \omega_p - 2\omega_l$.

When the pump cavity suffers a cavity decay, the dynamics of the system can be estimated by the master equation in the Lindblad form [48]

$$\dot{\rho} = i[\rho, \hat{H}_I] + \kappa_p \mathcal{L}(\hat{a}_p) \rho, \quad (3)$$

where for an arbitrary operator \hat{o} , the standard Lindblad superoperator is defined as

$$\mathcal{L}(\hat{o})\rho = \hat{o}\rho\hat{o}^\dagger - \frac{1}{2}(\hat{o}^\dagger\hat{o}\rho + \rho\hat{o}^\dagger\hat{o}). \quad (4)$$

Here, κ_p is the single-photon dissipation rate (i.e., the cavity decay rate) of the pump cavity. Due to the presence of the driving Ω of the pump mode, we first set $\hat{c}_p = \hat{a}_p + d$ to derive the effective Hamiltonian of the system. Thereafter, the Hamiltonian in Eq. (2) is transformed to

$$\begin{aligned} \hat{H}_h = & \delta_p(\hat{c}_p^\dagger - d^*)(\hat{c}_p - d) + \delta_s \hat{a}_s^\dagger \hat{a}_s + \delta_q \hat{S}_z \\ & + \left[J(\hat{c}_p - d)\hat{a}_s^{\dagger 2} + g \hat{a}_s \hat{S}_+ + \frac{\Omega^*}{2} \hat{c}_p + \text{H.c.} \right]. \end{aligned} \quad (5)$$

Meanwhile, the second term of the master equation in Eq. (3) becomes

$$\kappa_p \mathcal{L}(\hat{a}_p) \rho = \kappa_p \mathcal{L}(\hat{c}_p) \rho - i[\hat{H}_{\text{me}}, \rho], \quad (6)$$

where $\hat{H}_{\text{me}} = -i\kappa_p(d^* \hat{c}_p - d \hat{c}_p^\dagger)/2$. Then, the total Hamiltonian can be described as

$$\begin{aligned} \hat{H}_{\text{tot}} = & \hat{H}_h + \hat{H}_{\text{me}} \\ = & \delta_p \hat{c}_p^\dagger \hat{c}_p + \delta_s \hat{a}_s^\dagger \hat{a}_s + \delta_q \hat{S}_z - J(d \hat{a}_s^{\dagger 2} + d^* \hat{a}_s^2) \end{aligned}$$

$$+ \left(\Omega_d \hat{c}_p + J \hat{c}_p \hat{a}_s^{\dagger 2} + g \hat{a}_s \hat{S}_+ + \text{H.c.} \right), \quad (7)$$

and the dynamics of the system can be modelled by the master equation

$$\dot{\rho} = -i[\hat{H}_{\text{tot}}, \rho] + \kappa_p \mathcal{L}(\hat{c}_p)\rho, \quad (8)$$

where $\Omega_d = (\Omega^* - 2d^* \delta_p - i\kappa_p d^*)/2$. For simplicity, we have set $d = \Omega/(2\delta_p - i\kappa_p)$ to eliminate the driving term with Ω_d .

According to the second and fourth terms in Eq. (7), the signal cavity is squeezed [49–54]. Applying the Bogoliubov transformation [29, 52–56]

$$\hat{a}_s = \cosh(r) \hat{a}_s + \sinh(r) e^{i\theta_s} \hat{a}_s^\dagger,$$

one can diagonalize the signal-cavity Hamiltonian in Eq. (7), and obtain the Hamiltonian

$$\begin{aligned} \hat{\mathcal{H}} = & \delta_p \hat{c}_p^\dagger \hat{c}_p + \delta_s \hat{a}_s^\dagger \hat{a}_s + \delta_q \hat{S}_z \\ & + \left\{ J [\cosh(r) \hat{a}_s + \sinh(r) e^{i\theta_s} \hat{a}_s^\dagger]^2 \hat{c}_p^\dagger \right. \\ & \left. + g [\cosh(r) \hat{a}_s + \sinh(r) e^{i\theta_s} \hat{a}_s^\dagger] \hat{S}_+ + \text{H.c.} \right\}, \quad (9) \end{aligned}$$

where $\delta_s = \sqrt{\delta_s^2 - (2J|d|)^2}$, $\theta_s = -\arctan(\text{Im}(d)/\text{Re}(d))$, and $r = (1/4) \ln[(\delta_s + 2J|d|)/(\delta_s - 2J|d|)]$. Here, we set $\delta_s \gg 2J|d|$, which makes the cavity squeezing parameter r approach 0. Then, we have $\cosh(r) \rightarrow 1$, $\sinh(r) \rightarrow r$, and $\sinh(2r) \rightarrow 2r$. Thereafter, the Hamiltonian $\hat{\mathcal{H}}$ in Eq. (9) becomes approximated by

$$\begin{aligned} \hat{\mathcal{H}} \simeq & \delta_s \hat{a}_s^\dagger \hat{a}_s + \delta_q \hat{S}_z + \delta_p \hat{c}_p^\dagger \hat{c}_p \\ & + \left[J (\hat{a}_s + r e^{i\theta_s} \hat{a}_s^\dagger)^2 \hat{c}_p^\dagger + g (\hat{a}_s + r e^{i\theta_s} \hat{a}_s^\dagger) \hat{S}_+ + \text{H.c.} \right]. \quad (10) \end{aligned}$$

Furthermore, when the condition $\delta_s \gg \{J, g_c\}$ is satisfied, according to the works in Refs. [57, 58], the dynamics of the system can, up to the third order, be described by the effective Hamiltonian

$$\begin{aligned} \hat{\mathcal{H}}_{\text{eff}} = & \hat{\mathcal{H}}_{\text{eff}}^{(1)} + \hat{\mathcal{H}}_{\text{eff}}^{(2)} + \hat{\mathcal{H}}_{\text{eff}}^{(3)}, \\ \hat{\mathcal{H}}_{\text{eff}}^{(1)} = & \delta_p \hat{c}_p^\dagger \hat{c}_p + \delta_q \hat{S}_z + Jr(2\hat{a}_s^\dagger \hat{a}_s + 1)(e^{-i\theta_s} \hat{c}_p + \text{H.c.}), \\ \hat{\mathcal{H}}_{\text{eff}}^{(2)} = & -\frac{J^2}{2\delta_s} (2\hat{c}_p^\dagger \hat{c}_p + 4\hat{c}_p^\dagger \hat{c}_p \hat{a}_s^\dagger \hat{a}_s - \hat{a}_s^\dagger \hat{a}_s^\dagger \hat{a}_s \hat{a}_s) \\ & -\frac{g^2}{\delta_s} (2\hat{a}_s^\dagger \hat{a}_s \hat{S}_z + \hat{S}_+ \hat{S}_-), \\ \hat{\mathcal{H}}_{\text{eff}}^{(3)} = & \frac{g^2}{\delta_s} \left[\left(\frac{J}{\delta_s} \hat{c}_p + r e^{i\theta_s} \right) \hat{S}_+^2 + \text{H.c.} \right], \quad (11) \end{aligned}$$

where $\hat{\mathcal{H}}_{\text{eff}}^{(\mathcal{J})}$ ($\mathcal{J} = 1, 2, 3$) represents the \mathcal{J} th order processes of the effective Hamiltonian. Here, we also have neglected the fast-oscillating terms by the rotating wave approximation. Note that the Hamiltonian $\hat{\mathcal{H}}_{\text{eff}}^{(3)}$ in Eq. (11) contains the nonlinear interactions of the atomic

ensembles, which is crucial for generating spin squeezing in the protocol. However, these nonlinear interactions are third-order processes whose effect would be masked by that of the lower-order interactions.

To eliminate the influence of the lower-order interactions, we tune the parameters and make some proper assumptions as shown in the following. First, we assume that the signal cavity is well cooled so that the signal cavity is in the vacuum state, i.e., $\langle \hat{a}_s^\dagger \hat{a}_s \rangle \simeq 0$. Therefore, all the interactions involving $\hat{a}_s^\dagger \hat{a}_s$, like the terms $\hat{a}_p^\dagger \hat{a}_p \hat{a}_s^\dagger \hat{a}_s$ and $\hat{a}_s^\dagger \hat{a}_s \hat{S}_z$, can be neglected. Meanwhile, $\delta_p = J^2/\delta_s$ is set to eliminate the Stark shift of the pump cavity. Furthermore, we assume that in the ensemble, the number of excited atoms is much smaller than the total number of atoms. Under this condition, the spin operator \hat{S}_z can be divided into two parts, i.e.,

$$\hat{S}_z = -\frac{N}{2} + \Delta \hat{S}_z, \quad (12)$$

where $\Delta \hat{S}_z$ is a small fluctuation around the ground state. After substituting Eq. (12) into the relation $\hat{S}_z^2 - \hat{S}_z + \hat{S}_+ \hat{S}_- = N(N+1)/4$, we obtain (ignoring the constant terms)

$$\hat{S}_+ \hat{S}_- \simeq (N+1) \Delta \hat{S}_z = (N+1) \hat{S}_z. \quad (13)$$

This means that, when the atomic ensemble is in the low-excitation regime, the effect of the coupling $\hat{S}_+ \hat{S}_-$ is to produce a Stark shift given by $(N+1) \hat{S}_z$. Therefore, one can choose $\delta_q = (N+1)g^2/\delta_s$ to eliminate the influence of the term $\hat{S}_+ \hat{S}_-$ effectively. Meanwhile, the effect of this term can be eliminated completely by introducing an auxiliary atomic level and a driven optical cavity [59–61] (see more details in Appendix A). In the rest of paper and numerical simulations, we assume the effect of $\hat{S}_+ \hat{S}_-$ has been fully compensated and $\delta_q = 0$. Correspondingly, the effective Hamiltonian of the system becomes

$$\hat{\mathcal{H}}_{\text{eff}} \approx g_{\text{eff}} (\hat{c}_p - d) \hat{S}_+^2 + \frac{J^2}{\delta_s} d^* \hat{c}_p + \text{H.c.}, \quad (14)$$

where we have made the approximation $r \rightarrow J|d|/\delta_s$ and assumed $g_{\text{eff}} = g^2 J/\delta_s^2$. Then, by taking corresponding reverse transformations, one can convert the effective Hamiltonian in Eq. (14) back to the original frame and obtain

$$\hat{H}_{\text{eff}} = g_{\text{eff}} (\hat{a}_p \hat{S}_+^2 + \hat{a}_p^\dagger \hat{S}_-^2) + \left(\frac{\Omega^*}{2} \hat{a}_p + \frac{\Omega}{2} \hat{a}_p^\dagger \right). \quad (15)$$

Meanwhile, the effective Lindblad-type master equation in Eq. (8) becomes

$$\dot{\rho} = i[\rho, \hat{H}_{\text{eff}}] + \kappa_p \mathcal{L}(\hat{a}_p)\rho. \quad (16)$$

The first term in Eq. (15) indicates that the system involves a cavity-induced TAT-like interaction which can be used to generate spin squeezing [27]. The built-in mechanism is that when the pump cavity is in a coherent

state with $\langle \hat{a}_p \rangle = \beta$, the effective Hamiltonian in Eq. (15) can be approximated as

$$\hat{H}'_{\text{eff}} = g_{\text{eff}}(\beta \hat{S}_+^2 + \beta^* \hat{S}_-^2), \quad (17)$$

i.e., the TAT interaction. Moreover, the TAT model in Eq. (17) can be established through keeping the pump cavity in a state with $\langle \hat{a}_p \rangle \neq 0$ during the evolution. According to Eqs. (15) and (16), keeping the state in the pump cavity unchanged can be achieved effectively by increasing the ratio between Ω and g_{eff} . The detail is that for a larger ratio Ω/g_{eff} , the pump cavity stays in a coherent state with amplitude $d_0 = i\Omega/\kappa_p$ efficiently for a longer period (see below for numerical demonstrations). For convenience, we take the coherent state as the quasi-steady state of the pump cavity in the remaining of the text.

So far, we have considered a model, which contains only the photon loss of the pump mode. In reality, there always exists some dissipative processes for the atomic ensemble and the signal cavity. Here, we assume that the system suffers from dissipation induced by the ensemble collective dephasing, the atomic spontaneous emission, and the signal cavity single-photon loss. The dynamics of the system can therefore be described by the following master equation

$$\dot{\rho}_I = i[\rho_I, \hat{H}_I] + \left[\sum_{v=s,p} \kappa_v \mathcal{L}(\hat{a}_v) + \sum_{k=1}^N \gamma_s \mathcal{L}(\hat{\sigma}_k^-) + \gamma_c \mathcal{L}(\hat{S}_z) \right] \rho_I, \quad (18)$$

where ρ_I is the density operator under the full dynamics of the system. The parameters κ_s , γ_s , and γ_c are the single-photon loss rate of the signal cavity, the spontaneous emission rate of atoms, and the collective dephasing rate of the atomic ensemble, respectively. In general, the third term in Eq. (18), i.e., $\sum_{k=1}^N \gamma_s \mathcal{L}(\hat{\sigma}_k^-) \rho_I$, makes numerical simulations of a large-size ensemble dynamics extremely difficult because the demanded computation resources increase exponentially with the total number of atoms N . However, the system dynamics involves only the zero momentum mode of the atomic ensemble, and also does not mix it with other nonzero momentum modes. Thus according to Refs. [27, 29, 62, 63], the third term in Eq. (18) can be reduced to

$$\sum_k \mathcal{L}(\hat{\sigma}_k^-) \rho_I = \frac{1}{N} \mathcal{L}(\hat{S}_-) \rho_I. \quad (19)$$

Then, the full master equation in Eq. (18) becomes

$$\dot{\rho}_I = i[\rho_I, \hat{H}_I] + \left[\sum_{v=p,s} \kappa_v \mathcal{L}(\hat{a}_v) + \frac{\gamma_s}{N} \mathcal{L}(\hat{S}_-) + \gamma_c \mathcal{L}(\hat{S}_z) \right] \rho_I. \quad (20)$$

Accordingly, the effective master equation in Eq. (16) is transformed to

$$\dot{\rho}_{\text{eff}} = i[\rho_{\text{eff}}, \hat{H}_{\text{eff}}]$$

$$+ \left[\sum_{v=s,p} \kappa_v \mathcal{L}(\hat{a}_v) + \frac{\gamma_s}{N} \mathcal{L}(\hat{S}_-) + \gamma_c \mathcal{L}(\hat{S}_z) \right] \rho_{\text{eff}}, \quad (21)$$

where ρ_{eff} represents the density operator under the effective dynamics of the system. Note that, the part $\kappa_s \mathcal{L}(\hat{a}_s)$ in Eq. (16) can be subtracted since the signal cavity has been decoupled from the dynamics of the effective Hamiltonian in Eq. (15).

As demonstrated above, we have obtained the cavity-induced TAT-like interaction effectively, and the Lindblad-type master equation to simulate the dynamics of the system. These enable us to generate spin squeezing and study the properties of the generated spin squeezing under different decoherence noise sources.

III. GENERATING SPIN SQUEEZING

In this section, we investigate the generation of spin squeezing through theoretical analyses and numerical simulations. First, we need to introduce the spin squeezing parameter ξ_R^2 proposed by Wineland *et al.* [1, 5, 6]

$$\xi_R^2 = N \frac{\langle (\hat{\mathbf{S}} \cdot \mathbf{n}_\perp)^2 \rangle - \langle \hat{\mathbf{S}} \cdot \mathbf{n}_\perp \rangle^2}{|\langle \hat{\mathbf{S}} \rangle|^2}, \quad (22)$$

where $\hat{\mathbf{S}} = \hat{S}_x \mathbf{e}_x + \hat{S}_y \mathbf{e}_y + \hat{S}_z \mathbf{e}_z$ and \mathbf{e}_u ($u = x, y, z$) is the unit vector along the u direction. The unit vector \mathbf{n}_\perp is along the direction minimizing the numerator. The spin squeezing parameter represents the ratio of the fluctuations between a quantum state of interest and a coherent spin state (CSS) in Ramsey spectroscopy. Here, the CSS acts as a noise-reference state. It is seen from Eq. (22) that, when $\xi_R^2 < 1$, the phase sensitivity of the state of interest is improved over the standard quantum limit (SQL), i.e., this state is squeezed. Note that, a smaller ξ_R^2 indicates a stronger spin squeezing. In this paper, we choose the parameter ξ_R^2 to characterize the strength of the generated spin squeezing.

To numerically simulate the evolution of the system, we use the Monte Carlo approach (i.e., the quantum-jump method) [64], where individual quantum trajectories of the system evolve under a non-Hermitian Hamiltonian, and then are randomly interrupted by quantum jumps. Moreover, the dynamics of the system is regarded as an ensemble average over these trajectories of the system wave functions. The number of the involved trajectories is larger and the description on the dynamics of the system is more precise. However, simulating a large number of trajectories also requires many computation resources. Therefore, after balancing the precise of the numerical simulation and the requirement of the computation resources, we take the average over 1000 trajectories to calculate the dynamics of the system.

In the following two subsections, we assume that initially, the pump cavity is in a coherent state $|\alpha\rangle_p$,

where $\alpha = |\alpha|e^{i\varphi}$ is the complex amplitude with an argument $\varphi = \arg(\alpha)$. At the same time, the signal cavity and the atomic ensemble are well cooled to their ground states, i.e., $|0\rangle_s$ and $|l, -l\rangle_e$, respectively, where $l = N/2$. Here, $|j, m_z\rangle_e$ represents a collective spin state of an ensemble of N spin-1/2 atoms, with an orbital angular momentum quantum number and a magnetic quantum number $m_z \in \{-l, -l+1, \dots, l-1, l\}$.

A. WITH DRIVING THE PUMP CAVITY

In this subsection, we study the generation of spin squeezing in the case where the pump cavity is driven by external fields and is initialized in the quasi-steady coherent state, i.e., $\alpha = d_0 = i\Omega/\kappa_p$.

First, we assume that the dynamics of the system can be well described by the master equation in Eq. (3). From the discussion below Eq. (16), one can find that the strength of the generated spin squeezing is determined by the state of the pump cavity during the evolution. Therefore, the evolution of the pump cavity is worth studying. According to Eqs. (15) and (16), the pump cavity seems to stay in a coherent state effectively during the evolution when one sets $\{\kappa_p, \Omega\} \gg g_{\text{eff}}$. Thus, we introduce a coherent state $|\beta_p\rangle_p$ whose amplitude is $\beta_p \equiv \langle \hat{a}_p \rangle_p$ (time-dependent), as a reference state, and define the fidelity $F_{I(\text{eff})} = {}_p\langle \beta_p | \rho_{I(\text{eff})} | \beta_p \rangle_p$ to study the state of the pump cavity. From Fig. 2(a), we can observe that both F_I and F_{eff} are always greater than 0.995 within the evolution time of $t = 300/g_c$. In other words, the pump cavity stays in the coherent state effectively during the evolution. Therefore, according to Eq. (17), the dynamics of the ensemble can be well described by the TAT model if the pump cavity is initially in a coherent state. Therefore, the protocol could give rise to a strong squeezing strength. According to Fig. 2(b), we find that under the chosen parameters, the protocol is able to generate a spin squeezing of $\xi_R^2 \sim -9.24$ dB in an ensemble of $N = 50$ atoms.

Moreover, the squeezing direction is also an essential property of spin squeezing. From the cavity-induced TAT-like interaction and the initial coherent state of the pump cavity, $\langle \hat{S}_x \rangle = \langle \hat{S}_y \rangle = 0$ is maintained during the evolution of the system. Therefore, the mean-spin direction is along the z direction and the spin squeezing only occurs in the x - y plane. To find the spin squeezing direction \mathbf{n}_\perp , we randomly choose a direction of the x - y plane $\mathbf{n}_r = \cos\theta \mathbf{e}_x + \sin\theta \mathbf{e}_y$, where θ is the polar angle. As discussed above, the argument φ is maintained effectively during the evolution. According to Eq. (17) and Ref. [1], the squeezing direction \mathbf{n}_\perp satisfies $\theta = \pi/4 + \varphi/2$. Here, we demonstrate the spin squeezing direction at the moment where the strongest squeezing occurs (the dots in Fig. 2(b)). To show the spin squeezing direction intuitively, we introduce the Husimi- Q function which represents the quasiprobability distribution of any

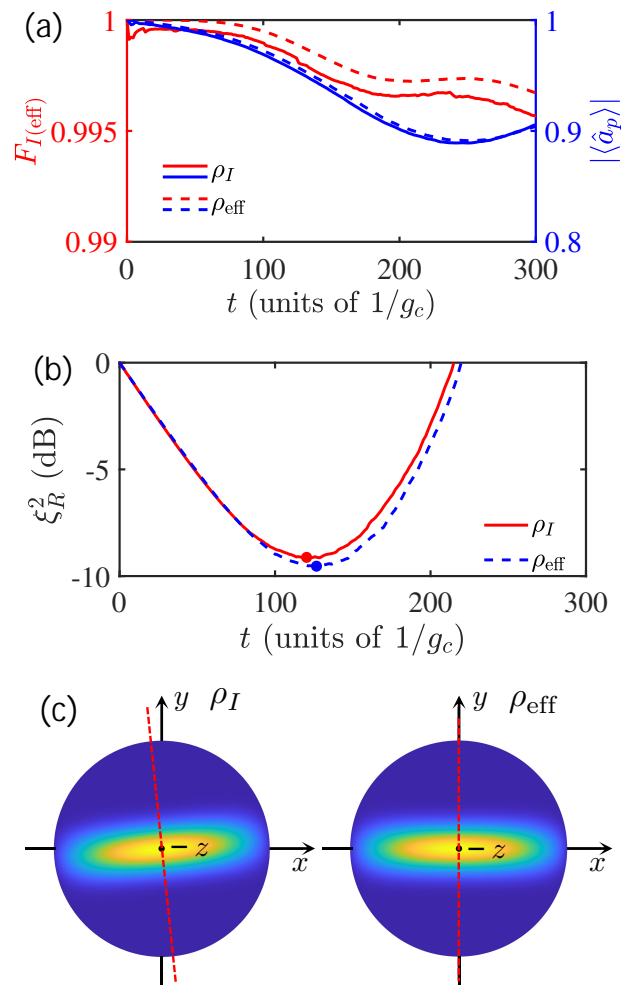


FIG. 2. Time evolution of (a) the parameters $F_{I(\text{eff})}$, $|\langle \hat{a}_p \rangle|$, and (b) the spin squeezing parameter ξ_R^2 , given by the full master equation in Eq. (20) (solid curve) and the effective master equation in Eq. (21) (dashed curve) for $\kappa_p = \Omega = g_c$. All other parameters are $N = 50$, $\delta_s = 15g_c$, $J = \sqrt{2}g_c$, and $\kappa_s = \gamma_c = \gamma_s = 0$. (c) Husimi- Q function and spin squeezing direction (red dashed line) for the strongest spin squeezing (corresponding to the dots in (b)). Here, ρ_I and ρ_{eff} represent the states given by the full master equation in Eq. (20) and the effective master equation in Eq. (21), respectively.

spin states [1]. The Husimi- Q function is defined as

$$Q_{I(\text{eff})} = \langle \text{CSS} | \hat{R}^\dagger(\theta_Q, \phi_Q) \rho_{I(\text{eff})} \hat{R}(\theta_Q, \phi_Q) | \text{CSS} \rangle,$$

where $|\text{CSS}\rangle$ represents a CSS with all the atoms in their excited states and $\hat{R}(\theta_Q, \phi_Q) = \exp[i\theta_Q(\hat{S}_x \sin\phi_Q - \hat{S}_y \cos\phi_Q)]$ is a rotation operator [1]. From Fig. 2(c), we find that the spin squeezing direction under the full dynamics of the system deviates slightly from the effective prediction (i.e., y axis). In other words, the analysis about the spin squeezing direction is effective. Moreover, from Figs. 2(a-c), we have demonstrated the validity of the effective master equation to describe the dynamics of the full system. These results show that the

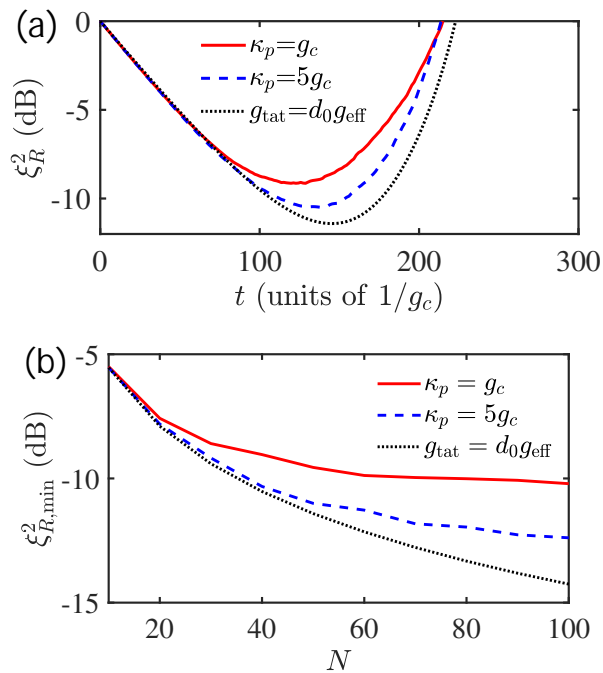


FIG. 3. (a) Time evolution of the spin squeezing parameter ξ_R^2 for an ensemble of $N = 50$ atoms, given by the full master equation in Eq. (20). (b) Minimum values of the spin squeezing parameter $\xi_{R,\min}^2$ for different N , given by the effective master equation in Eq. (21). We assumed that $\kappa_p = g_c$ (red solid curve) and $\kappa_p = 5g_c$ (blue dashed curve) for the present protocol, and that $g_{\text{tat}} = d_0 g_{\text{eff}} = ig_{\text{eff}}$ (black dotted curve) for the TAT protocol. Other parameters are $\Omega = \kappa_p$, $\delta_s = 15g_c$, $J = \sqrt{2}g_c$, and $\kappa_s = \gamma_c = \gamma_s = 0$.

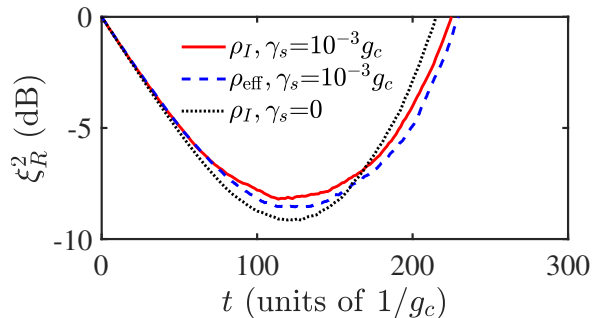


FIG. 4. Time evolution of the spin squeezing parameter ξ_R^2 for different γ_s . The involved spontaneous emission rates γ_s are set to be: $10^{-3}g_c$ (for ρ_I , red solid curve, and for ρ_{eff} , blue dashed curve) and 0 (for ρ_I , black dotted curve). All other parameters are same as those in Fig. 2.

assumptions and the approximations we have made in Sec. II are suitable.

According to the mechanism of the cavity-induced TAT-like interaction in Sec. II, when the condition $\{\kappa_p, \Omega\} \gg g_{\text{eff}}$ is satisfied, the dynamics of the system is consistent with that of the TAT model. To confirm this, we now introduce the TAT protocol, as a reference.

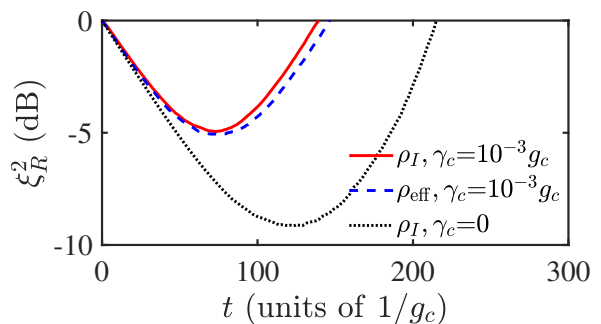


FIG. 5. Time evolution of the spin squeezing parameter ξ_R^2 for different γ_c . The involved dephasing rates γ_c are set to be: $10^{-3}g_c$ (for ρ_I , red solid curve, and for ρ_{eff} , blue dashed curve) and 0 (for ρ_I , black dotted curve). All other parameters are same as those in Fig. 2.

The Hamiltonian in the TAT protocol is given by

$$\hat{H}_{\text{TAT}} = g_{\text{tat}} \hat{S}_+^2 + g_{\text{tat}}^* \hat{S}_-^2, \quad (23)$$

where $g_{\text{tat}} = d_0 g_{\text{eff}}$. Compared to the present protocol, the TAT protocol is equivalent to a case where the pump cavity stays in the quasi-steady state during the evolution. Thereafter, we numerically compare the present protocol and the TAT protocol. Figure 3(a) plots the evolution of ξ_R^2 verse t , showing that a larger κ_p increases the similarity between the present protocol and the TAT protocol. In particular, all the curves are in clear agreement with each other at the beginning of the evolution. The reason is that, from Fig. 2(a), we can obtain that the pump cavity is in the quasi-steady state effectively at the beginning of the evolution. From Fig. 3(b), one can find that for a small ensemble, the present protocol can generate the same spin squeezing strength as the TAT protocol, e.g., $\Omega = \kappa_p = 5g_c$ for $N = 10$. Moreover, it is also seen that, as the number of atoms increases, the minimum value of the spin squeezing parameter $\xi_{R,\min}^2$ is decreased for both the present protocol and the TAT protocol. However, an increasing in the number of atoms causes the strongest spin squeezing generated with the present protocol to gradually deviate from that generated with the TAT protocol. The reason is that the generation of spin squeezing in an ensemble with more atoms generally leads more atoms to be excited, which would cause the state of the pump cavity to deviate more from the quasi-steady coherent state. Moreover, according to Figs. 3(a) and 3(b), a larger κ_p results in a stronger spin squeezing. This means that a setup with a larger single-photon dissipation of the pump cavity and a stronger external driving field is more efficient for the present protocol to generate a stronger spin squeezing.

Then, we study the influence of the spontaneous emission of the atoms and the collective dephasing of the ensemble. From Fig. 4, we find that the effect of spontaneous emission prolongs the duration of the squeezing at the expense of reducing the squeezing

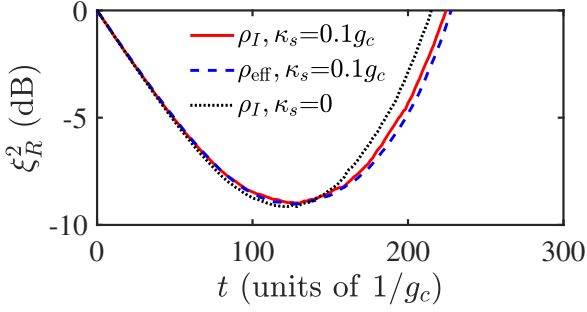


FIG. 6. Time evolution of the spin squeezing parameter ξ_R^2 for different κ_s . The involved signal cavity decay rates κ_s are set to be: $0.1g_c$ (for ρ_I , red solid curve, and for ρ_{eff} , blue dashed curve) and 0 (for ρ_I , black dotted curve). All other parameters are same as those in Fig. 2.

strength slightly. Meanwhile, it can be seen from Fig. 5 that, at the same intensity, the influence of the collective dephasing of the ensemble on the generated spin squeezing is much greater than that caused by the atomic spontaneous emission. The essential reason is that the collective dephasing would affect the relative phases between the energy levels of the ensemble, so that the direction of the squeezing gradually becomes chaotic during the evolution.

Though the signal cavity is decoupled from the effective dynamics described by Eq. (21), the signal cavity decay affects inevitably the full dynamics of the system in reality. Here, we discuss the influence of the signal cavity decay on the system. With the help of the theory of the adiabatic elimination [65, 66], we can replace $\gamma_s \mathcal{L}(\hat{a}_s)\rho$ with $J^2 p_\gamma \mathcal{L}(\hat{a}_p)\rho + g^2 p_\gamma \mathcal{L}(\hat{S}_-)\rho$, where $p_\gamma = 4\gamma_s / (4\delta_s^2 + \gamma_s^2)$, in the master equation in Eqs. (20) and (21) (see more details in Appendix B). Therefore, the effect of the signal cavity decay causes an additional single-photon dissipation of the pump cavity and an additional collective spontaneous emission of the atoms. From Sec. II, the condition $\kappa_p \gg J^2 p_\gamma$ is well satisfied, which means that the adiabatic effect on the pump cavity may be not obvious. Then, the signal cavity decay mainly produces an additional collective spontaneous emission. This analysis can be verified indirectly by comparing the evolution of the spin squeezing parameter ξ_R^2 in Figs. 4 and 6.

B. WITHOUT DRIVING THE PUMP CAVITY

In this subsection, we discuss the property of the generated spin squeezing without driving the pump cavity. Here, the effective Hamiltonian in Eq. (15) is given by

$$\hat{H}'_{\text{eff}} = g'_{\text{eff}}(\hat{a}_p \hat{S}_+^2 + \hat{a}_p^\dagger \hat{S}_-^2), \quad (24)$$

where $g'_{\text{eff}} = g^2 J / \delta_s^2$.

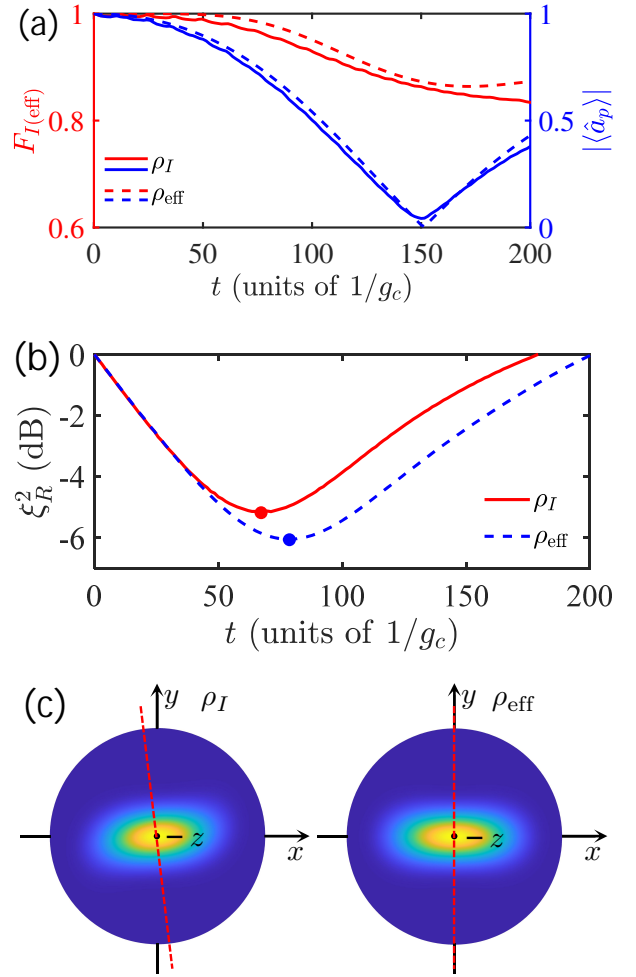


FIG. 7. Time evolution of (a) the parameters $F_{I(\text{eff})}$, $|\langle \hat{a}_p \rangle|$, and (b) the spin squeezing parameter ξ_R^2 , given by the full master equation in Eq. (20) (the solid curve) and the effective master equation in Eq. (21) (the dashed curve) for $\alpha = i$. All other parameters are $N = 50$, $\delta_s = 15g_c$, $J = \sqrt{2}g_c$, and $\Omega = \kappa_p = \kappa_s = \gamma_c = \gamma_s = 0$. (c) Husimi- Q function and spin squeezing direction (the red dashed curve) for the strongest spin squeezing (corresponding to the dots in (b)).

First, we study the generation of spin squeezing in the ideal case of no decoherence involved. Similar to the Sec. III A, we start from studying the coherence properties of the pump cavity with a coherent state as a reference state. Without the driving, the amplitude of the reference state is decreased sharply in the early stage, as shown in Fig. 7(a). This indicates that the initial coherent state of the pump cavity is destroyed, which, according to Eq. (17), limits the strength of the generated spin squeezing. As shown in Fig. 7(b), the protocol is able to generate a spin squeezing of $\xi_R^2 \sim -5.19$ dB in an ensemble of $N = 50$ atoms. Meanwhile, from Figs. 7(a) and 7(b), we find that the fidelity of the reference coherent state exceeds 0.98 before the strongest squeezing occurs. In other words, the pump cavity is in a coherent state approximately. Therefore, the prediction

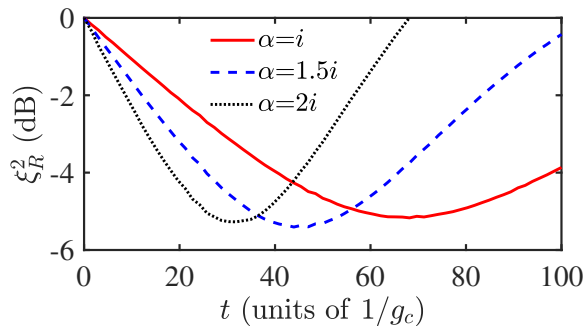


FIG. 8. Time evolution of the spin squeezing parameter ξ_R^2 for different α , given by the full master equation in Eq. (20). The involved amplitudes of the initial coherent state α are set to be: i (red solid curve), $1.5i$ (blue dashed curve), and $2i$ (black dotted curve). All other parameters are same as those in Fig. 7.

of the spin squeezing direction along $\theta = \pi/4 + \varphi/2$ in the x - y plane is still valid. From Fig. 7(c), the spin squeezing direction based on the full master equation only has a small deviation from the effective prediction (i.e., along the y axis). Moreover, from Figs. 7(a) and 7(c), the effective master equation is also still valid to describe the system dynamics. However, the effective master equation, when used to predict the evolution of ξ_R^2 , has a big deviation due to the sensitivity of ξ_R^2 to the parameters. Therefore, the following numerical simulations in this subsection are all based on the full master equation.

According to Figs. 7(a) and 7(b), an increase in the amplitude of the initial coherent state of the pump cavity might lead to a faster and stronger spin squeezing. Here, we numerically study this deduction and plot the corresponding results in Fig. 8. From Fig. 8, a larger-amplitude coherent state prepared in the pump cavity accelerates the process of generating spin squeezing. The reason is that according to Eq. (17), an increase in the amplitude of the coherent state in the pump cavity increases the coupling strength of the nonlinear interaction between the atoms. But at the same time, a larger-amplitude coherent state in the pump cavity also involves a violation of the assumption $\delta_s \gg 2|\alpha|J$. This results in a decrease of the generated squeezing strength, as shown in Fig. 8.

It is worth studying further the effects of the spontaneous emission of the atoms and the collective dephasing of the ensemble on the system. As shown in Fig. 9, the spontaneous emission of the atoms slightly influence on the evolution of spin squeezing. Compared to the case with driving the pump cavity in Sec. III A, the atomic spontaneous emission cannot prolong the duration of spin squeezing in the case of no pump cavity driving. According to Figs. 9 and 10, when setting $\gamma_s = \gamma_c$, the dephasing of the ensemble has a greater effect on the generation of spin squeezing than the atomic spontaneous emission. Meanwhile, from Figs. 5 and 10, it

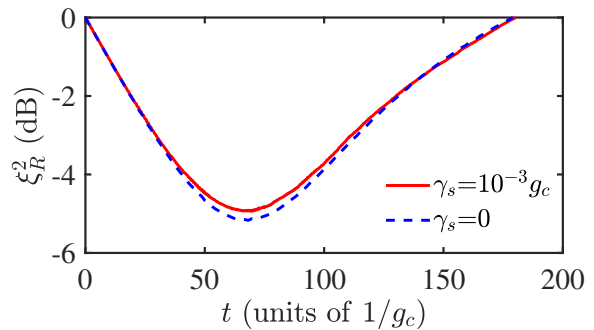


FIG. 9. Time evolution of the spin squeezing parameter ξ_R^2 for different γ_s , given by the full master equation in Eq. (20). The involved atomic spontaneous emission rates γ_s are set to be: $10^{-3}g_c$ (red solid curve) and 0 (blue dashed curve). All other parameters are same as those in Fig. 7.

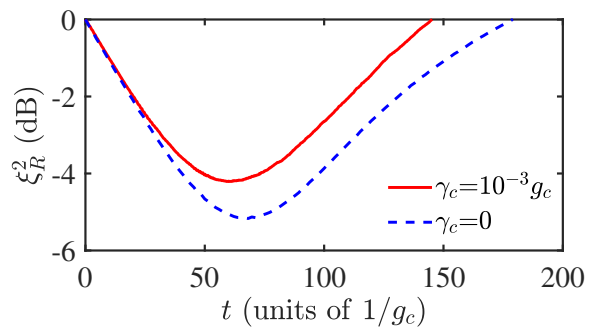


FIG. 10. Time evolution of the spin squeezing parameter ξ_R^2 for different γ_c , given by the full master equation in Eq. (20). The involved collective dephasing rates γ_c are set to be: $10^{-3}g_c$ (red solid curve) and 0 (blue dashed curve). All other parameters are same as those in Fig. 7.

can be found that in the case of no pump cavity driving, the collective dephasing of the ensemble has a weaker influence on the generation of spin squeezing than that in the case with driving the pump cavity.

Furthermore, the effect of the cavity decay on the system also needs to be investigated. Here, the pump cavity decay becomes an undesired physical process. According to Fig. 11, the pump cavity decay can significantly prolong the duration of squeezing, but at the same time, it can also clearly reduce the strength of squeezing. This indicates that the protocol in the case without driving the pump cavity is particularly suitable for a system with a high-quality pump cavity. Meanwhile, as discussed in Sec. III A, the influence of the signal cavity decay is equivalent to introducing an extra pump cavity decay and an extra atomic collective spontaneous emission. It is worth noting that the extra pump cavity decay cannot be ignored like in the case with driving the pump cavity. Thus, the robustness of the generated spin squeezing to the signal cavity decay would be reduced, which is shown in Fig. 12.

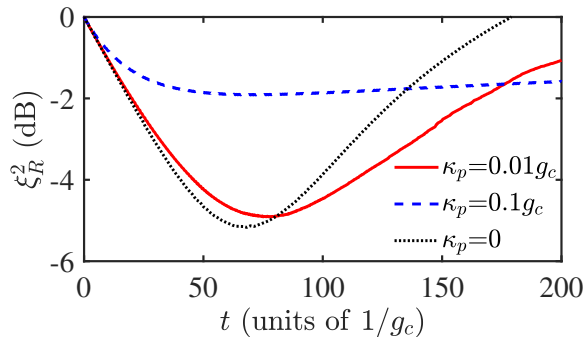


FIG. 11. Time evolution of the spin squeezing parameter ξ_R^2 for different κ_p , given by the full master equation in Eq. (20). The involved single-photon dissipation rates of the pump cavity κ_p are set to be: $0.01g_c$ (red solid curve), $0.1g_c$ (blue dashed curve), and 0 (black dotted curve). All other parameters are same as those in Fig. 7.

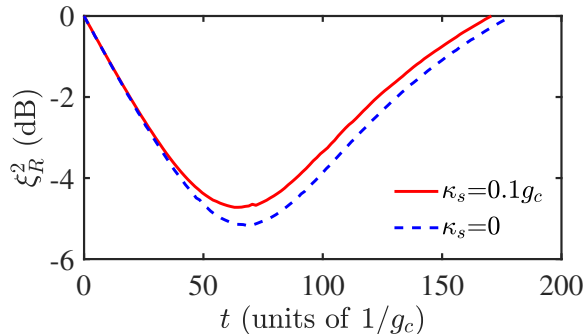


FIG. 12. Time evolution of the spin squeezing parameter ξ_R^2 for different κ_s , given by the full master equation in Eq. (20). The involved single-photon dissipation rates of the signal cavity κ_s are set to be: $0.1g_c$ (red solid curve) and 0 (blue dashed curve). All other parameters are same as those in Fig. 7.

IV. EXPERIMENTAL FEASIBILITY

In order to demonstrate further the performance of the protocol, we discuss the experimental feasibility by combining the theoretical model in the protocol with the current experiments.

Here, we consider that a setup consisting of two coplanar waveguide resonators (CPWRs), a superconducting quantum interference device (SQUID), and a rubidium (Rb) atomic ensemble, as shown in Fig. 13. The SQUID is used to mediate the parametric conversion between a single photon of the pump cavity (CPWR I) and a pair of photons of the signal cavity (CPWR II). In other words, the SQUID constructs the parametric coupling between two cavities. The pumping frequency of the SQUID satisfies $\omega_{\text{SQUID}} = 2\omega_s - \omega_p$. The SQUID has been designed and realized in many experiments, like the asymmetrically threaded SQUID (ATS) [37] and the rf-SQUID [38].

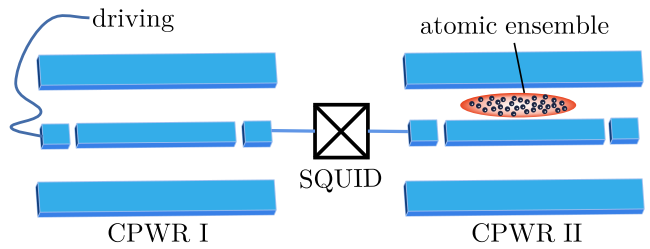


FIG. 13. Schematic for a possible architecture for the protocol. The CPWR I and the CPWR II are coupled to the SQUID. The atomic ensemble is placed above the CPWR II and is coupled to the magnetic mode of the CPWR II. An extra driving is applied to the CPWR I.

The strength of the parametric coupling constructed by the SQUID has been reported with a range of $J/2\pi = 0.1 \sim 17.7$ MHz [35–38]. Meanwhile, we take the atomic clock states $\{5S^{1/2}, F = 1, m_F = -1\} := |1, -1\rangle$ and $\{5S^{1/2}, F = 2, m_F = 1\} := |2, 1\rangle$ as the information carrier [39, 40]. To date, coupling these two states to the CPWR has been experimentally implemented with an additional rf field [39]. However, the reported coupling strength is too weak to implement efficient quantum coherent operations [41]. Fortunately, several approaches can be used to increase the coupling strength. Such approaches include decreasing the space between the atomic ensemble and the CPWR [39], and introducing novel CPWRs of being able to provide some strong magnetic fields [42]. Thus, here, we take $g_c/2\pi = 40$ kHz with $N = 10^6$ [40]. Note that, both the relaxation time T_1 and the coherent time T_2 of the Rb atomic ensemble are of the order sec [43]. This indicates that one can ignore the effect of the atomic spontaneous emission and the collective dephasing on the dynamics of the system. In addition, for the CPWRs, the quality factor over 10^6 has been realized experimentally [44–46]. Thus, we take $\kappa_p \sim 10^{-6}\omega_p$ and $\kappa_s \sim 10^{-6}\omega_s$. According to these parameters mentioned above, we list a group of feasible parameters and then estimate the minimum of the spin squeezing parameter in Table I. Note that, for the case with driving (discussed in Sec. III A), it is not necessary that the initial state of the pump cavity is the quasi-steady coherent state. As shown in Fig. 14, the generation of spin squeezing is also able to be achieved when the pump cavity is in the ground state initially. Meanwhile, from Fig. 14, one can find that the generations of spin squeezing between these two cases with different initial states of the pump cavity are almost the same. The reason of this similarity is that the time cost of constructing the quasi-steady coherent state from the ground state in the pump cavity is too short to change the generation of spin squeezing significantly.

Furthermore, the protocol can also be implemented with ensembles of other particles, such as nitrogen-vacancy (NV) centers in diamond [67–77]. In this case, a feasible setup is the same as the one shown in Fig. 13, but with replacing the atomic ensemble by the NV centers.

TABLE I. Experimental feasible parameters and the minimum of spin squeezing parameters

Parameter	Type of ensemble					
	Rb atoms			NV centers		
encoded states	$ 1, -1\rangle \leftrightarrow 2, 1\rangle$			$ m_s = 0\rangle \leftrightarrow m_s = -1\rangle$		
number of spins	10^6			10^{12}		
spin frequency $\omega_q/2\pi$ (GHz)	6.8324			2.6899		
spin spontaneous emission rate $\gamma_s/2\pi$ (kHz)	—			—		
spin collective dephasing rate $\gamma_c/2\pi$ (kHz)	—			0.26		
collective coupling strength $g_c/2\pi$ (kHz)	40			1.200×10^4		
signal cavity frequency $\omega_s/2\pi$ (GHz)	6.8330			2.8691		
signal cavity decay rate $\kappa_s/2\pi$ (kHz)	7			3		
parameter coupling strength $J/2\pi$ (kHz)	56.569			1.697×10^4		
SQUID's pumping frequency $\omega_{\text{SQUID}}/2\pi$ (GHz)	10			2		
pump cavity frequency $\omega_p/2\pi$ (GHz)	3.6660			3.7389		
external field	driving	driving	no driving	driving	driving	no driving
driving amplitude $\Omega/2\pi$ (MHz)	10	10	—	10	10	—
pump cavity decay rate $\kappa_p/2\pi$ (MHz)	10	10	0.003	10	10	0.003
amplitude of the initial coherent state α	0	i	i	0	i	i
minimum of the spin squeezing parameter $\xi_{\mathcal{R},\min}^2$ (dB) ¹	-15.13	-14.91	-2.34	-13.58	-13.58	-9.51

¹ Parameter $\xi_{\mathcal{R},\min}^2$ differs from the parameter $\xi_{R,\min}^2$ in Sec. III. The details are shown in Appendix C.

We encode the internal states of the NV centers, $|m_s = 0\rangle$ and $|m_s = -1\rangle$, as the information carrier [71]. The coupling strength between a single NV center and a single CPWR photon $g/2\pi$ exceeds 12 Hz [67, 71]. To date, for a typical ensemble of NV centers, the relaxation time of $T_1 \sim 40$ s ($\gamma_s \ll 1$ Hz) have been demonstrated experimentally [67] and, with the spin-echo sequences, the coherent time of $T_2 > 600 \mu\text{s}$ ($\gamma_c < 0.26$ kHz) has also been reached [29, 72]. Thus, we also give a group of feasible parameters and the minimum of the spin squeezing parameter in Table I.

V. CONCLUSIONS

In this paper, we have proposed a protocol to generate spin squeezing in atomic ensembles via a fully quantum degenerate parametric amplifier. By adjusting the parameters, an effective cavity-induced TAT-like interaction can be achieved. The strength of the generated spin squeezing is determined by some properties of the pump cavity, such as the initial state, the driving strength, and the cavity decay. We mainly discuss the generated spin squeezing in two cases of the pump cavity. For the first case, the pump cavity is initially in the quasi-steady coherent state by a driving field and the cavity decay. Meanwhile, for the second case, the pump cavity is initiated in an arbitrary coherent state and there is no pump cavity driving.

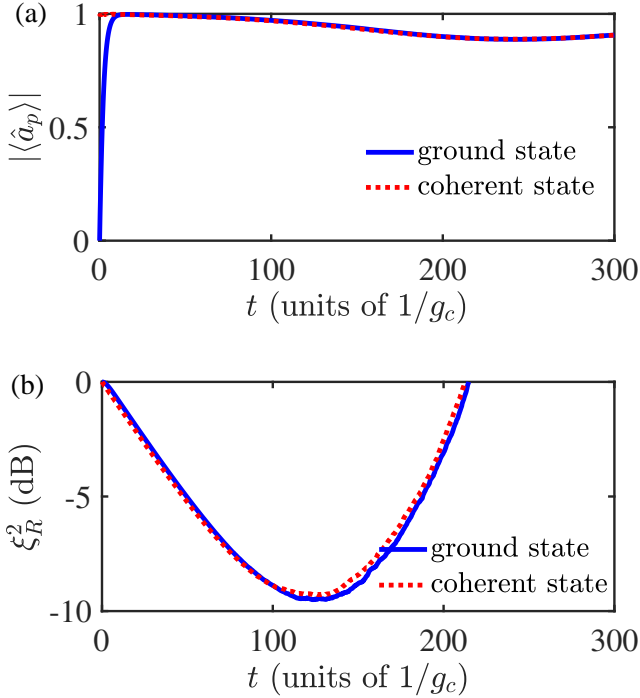


FIG. 14. Time evolution of (a) the parameter $|\langle \hat{a}_p \rangle|$, and (b) the spin squeezing parameter ξ_R^2 for the pump cavity initiated in the ground state (the blue solid curve) and the quasi-steady state (the red dotted curve), given by the full master equation in Eq. (20). All other parameters are $N = 50$, $\delta_s = 15g_c$, $\Omega = \kappa_p$, $J = \sqrt{2}g_c$, and $\kappa_s = \gamma_c = \gamma_s = 0$.

In the first case, theoretical analyses and numerical simulations show that the present protocol can generate a strong spin squeezing whose strength is even comparable to that of the TAT model. The reason is that, for a fixed d_0 and an extremely large ratio of κ_p to g_{eff} , the effect of the cavity-induced TAT-like interaction is equivalent to applying the TAT interaction to the atomic ensemble. Meanwhile, according to numerical simulations, the present protocol is robust to the atomic spontaneous emission and the signal cavity decay.

In the second case, according to numerical simulations, the present protocol can generate an observable spin squeezing. A properly large amplitude of the initial coherent state can accelerate the generation of spin squeezing. Meanwhile, the present protocol is also robust to the collective dephasing of the ensemble, in addition to the atomic spontaneous emission and the signal cavity decay. It is worth noting that the pump cavity decay is able to prolong the duration of squeezing significantly.

After combining the experimental results, we show that the present protocol is feasible experimentally. A group of realistic parameters, as shown in Table I, has been given to predict some experimentally feasible results. Moreover, the present protocol can be extended to generate spin squeezing in various ensembles, like ensembles of NV centers. We hope that the present

protocol provides a novel approach for generating spin squeezing in photon-spin coupling systems.

ACKNOWLEDGMENTS

This work was supported by the National Natural Science Foundation of China under Grants No. 11575045, No. 11874114, and No. 11674060, the Natural Science Funds for Distinguished Young Scholar of Fujian Province under Grant No. 2020J06011 and Project from Fuzhou University under Grant No. JG202001-2. Y.-H.C. was supported by the Japan Society for the Promotion of Science (JSPS) KAKENHI Grant No. JP19F19028. W.Q. is supported in part by the Incentive Research Project of RIKEN.

Appendix A. THE APPROACH FOR COMPENSATING THE TERM $(g^2/\delta_s)\hat{S}_+\hat{S}_-$ COMPLETELY

In this appendix, we give the detailed derivation of the approach for compensating $(g^2/\delta_s)\hat{S}_+\hat{S}_-$ completely. We first assume the information of spin squeezing is carrier by the levels of the atoms $|0\rangle_a \equiv |\downarrow\rangle_a$ and $|1\rangle_a \equiv |\uparrow\rangle_a$. Here, we introduce an optical cavity, a laser pulse, and an auxiliary level of the atoms $|2\rangle_a$ [59–61]. The optical cavity (pulse) is far-off resonant with the transition $|0\rangle_a \leftrightarrow |2\rangle_a$ ($|1\rangle_a \leftrightarrow |2\rangle_a$) with the coupling strength g_d (Ω_o) and the detuning Δ_d (Δ_o). In the interaction picture, the Hamiltonian described these interactions is given as

$$\hat{H}_o = \Delta_d \hat{d}^\dagger \hat{d} + g_c \sum_{k=1}^N (|2\rangle_{aa}^{kk} \langle 0| \hat{c} + |0\rangle_{aa}^{kk} \langle 2| \hat{c}^\dagger) + \Omega_o \sum_{k=1}^N (|2\rangle_{aa}^{kk} \langle 1| e^{-i\Delta_o t} + |1\rangle_{aa}^{kk} \langle 2| e^{i\Delta_o t}), \quad (\text{A1})$$

where \hat{d}^\dagger and \hat{d} are the creation operator and the annihilation operator of the optical cavity mode, respectively. $|\varepsilon\rangle_a^k$ ($\varepsilon = 0, 1, 2$ and $k = 1, 2, \dots, N$) represents that the k th atom is in $|\varepsilon\rangle_a$. When the conditions $\Delta_o - \Delta_d = \Delta$ and $\{\Delta_d, \Delta_o\} \gg \{g_d, \Omega_o, \Delta\}$ are satisfied, the auxiliary level $|2\rangle_a$ can be eliminated adiabatically and then the effective Hamiltonian of the system is

$$\hat{H}_{o,\text{eff}}^{(1)} = \frac{g_d \Omega_o}{\Delta'} \sum_{k=1}^N (|1\rangle_{aa}^{kk} \langle 0| \hat{d} e^{i\Delta t} + |0\rangle_{aa}^{kk} \langle 1| \hat{d}^\dagger e^{-i\Delta t}) + \frac{\Omega_o^2}{\Delta_o} \sum_{k=1}^N |1\rangle_{aa}^{kk} \langle 1| + \frac{g_d^2}{\Delta_d} \sum_{k=1}^N |0\rangle_{aa}^{kk} \langle 0| \hat{c}^\dagger \hat{c}, \quad (\text{A2})$$

where $\Delta' = 2\Delta_d \Delta_o / (\Delta_o + \Delta_d)$. To adiabatically eliminate the optical cavity mode, we set $\Delta \gg g_d \Omega_o / \Delta'$.

Then, the above effective Hamiltonian in Eq. (A2) is reduced to

$$\hat{H}_{o,\text{eff}}^{(2)} = \frac{g_d^2 \Omega_o^2}{\Delta'^2 \Delta} \hat{S}_+ \hat{S}_- + \frac{\Omega_o^2}{\Delta_o} \hat{S}_z, \quad (\text{A3})$$

where $\hat{S}_+ \hat{S}_- = \sum_{k=1}^N \sum_{k'=1}^N (|1\rangle_{aa}^{kk} \langle 0|) (|0\rangle_{aa}^{k'k'} \langle 1|)$ and $\hat{S}_z = 1/2 \sum_{k=1}^N (|1\rangle_{aa}^{kk} \langle 1| - \sum_{k=1}^N |0\rangle_{aa}^{kk} \langle 0|)$. This means that, when one takes

$$\frac{g_d^2 \Omega_o^2}{\Delta'^2 \Delta} + \frac{g^2}{\delta_s} = \delta_q + \frac{\Omega_o^2}{\Delta_o} = 0, \quad (\text{A4})$$

the effect of the undesired term $(g^2/\delta_s) \hat{S}_+ \hat{S}_-$ is compensated completely.

Appendix B. THE ADIABATIC ELIMINATION OF THE SIGNAL CAVITY

Due to few photons and strong cavity loss, the signal cavity can be considered as an ambience and can be adiabatically eliminated. Here, we give a detailed derivation on the adiabatic elimination of the signal cavity. According to the Hamiltonian in Eq. (2), one can obtain the interactions which excite signal cavity photons

$$\hat{V}_1 = J \hat{a}_p \hat{a}_s^{\dagger 2}, \quad \hat{V}_2 = g \hat{S}_- \hat{a}_s^{\dagger}, \quad (\text{B1})$$

and the free Hamiltonian of signal cavity photons

$$\hat{H}_e = \delta_s \hat{a}_s^{\dagger} \hat{a}_s. \quad (\text{B2})$$

We introduce a Lindblad operator $L_s = \sqrt{\gamma_s} \hat{a}_s$ which satisfies $\mathcal{L}(L_s)\rho = \gamma_s \mathcal{L}(\hat{a}_s)\rho$. According to the work in Ref. [65], the Lindblad operators of the effective master equation can be described as

$$\hat{L}_h = \hat{L}_s \left(\hat{H}_e - \frac{i}{2} \hat{L}_s^{\dagger} \hat{L}_s \right)^{-1} \hat{V}_h, \quad (\text{B3})$$

where, $h = 1, 2$. Then, one would obtain

$$\begin{aligned} \hat{L}_1 &= \frac{2\sqrt{\gamma_s} J}{2\delta_s - i\gamma_s} \hat{a}_p \hat{a}_s^{\dagger}, \\ \hat{L}_2 &= \frac{2\sqrt{\gamma_s} g}{2\delta_s - i\gamma_s} \hat{S}_-. \end{aligned} \quad (\text{B4})$$

This means that the Lindblad superoperator which describes the signal cavity decay $\gamma_s \mathcal{L}(\hat{a}_s)\rho$ can be replaced by $J^2 p_\gamma \mathcal{L}(\hat{a}_p \hat{a}_s^{\dagger})\rho + g^2 p_\gamma \mathcal{L}(\hat{S}_-)\rho$, where $p_\gamma = 4\gamma_s/(4\delta_s^2 + \gamma_s^2)$. Moreover, since the signal cavity remains in vacuum during the evolution of the system effectively, the term $J^2 p_\gamma \mathcal{L}(\hat{a}_p \hat{a}_s^{\dagger})\rho$ is able to reduce to $J^2 p_\gamma \mathcal{L}(\hat{a}_p)\rho$. Therefore, the effect of the signal cavity decay $\gamma_s \mathcal{L}(\hat{a}_s)\rho$ is equivalent to introducing an extra pump cavity decay $J^2 p_\gamma \mathcal{L}(\hat{a}_p)\rho$ and an extra atomic collective spontaneous

emission $g^2 p_\gamma \mathcal{L}(\hat{S}_-)\rho$. The physics mechanics is that, when the signal cavity is eliminated adiabatically, the pump cavity and the ensemble can be considered to be coupled to a new vacuum bath (i.e., the vacuum signal cavity).

Appendix C. THE MINIMUM OF THE SPIN SQUEEZING PARAMETER IN TABLE I

Note that, in typical ensembles, the number of particles is of the order of millions (e.g., Rb atoms) or trillions (e.g., NV centers). This means that it is extremely difficult to exactly estimate the full dynamics of the ensemble. In the following, we simplify the dynamics of the system and then obtain the minimum of spin squeezing effectively. With the Holstein-Primakoff transformation (HPT) [78] and in the limit of $N \rightarrow \infty$, the collective spin operators can be transformed to the bosonic operators as

$$\hat{S}_- \rightarrow \sqrt{N} \hat{b}, \quad \hat{S}_z \rightarrow -N/2 + \hat{b}^{\dagger} \hat{b}, \quad (\text{C1})$$

where \hat{b} is the bosonic annihilation operator. Accordingly, the spin squeezing parameter in Eq. (22) is rewritten as

$$\xi_{\mathcal{R}}^2 = \frac{N^2}{(N - 2\langle \hat{b}^{\dagger} \hat{b} \rangle)^2} (1 + 2\langle \hat{b}^{\dagger} \hat{b} \rangle - 2|\langle \hat{b}^2 \rangle|). \quad (\text{C2})$$

Meanwhile, from the effective master equation in Eq. (21) and the HPT, we obtain the Heisenberg equation [27]

$$\partial_t \hat{a}_p = -iN g_{\text{eff}} \hat{b}^2 - i\Omega^*/2 - (\kappa_p + J^2 p_\gamma) \hat{a}_p / 2, \quad (\text{C3a})$$

$$\partial_t \hat{b}^2 = -2iN g_{\text{eff}} \hat{a}_p (2\hat{b}^{\dagger} \hat{b} + 1) - (\gamma_s + g_c^2 p_\gamma + 2\gamma_c) \hat{b}^2, \quad (\text{C3b})$$

$$\partial_t \hat{b}^{\dagger} \hat{b} = -2iN g_{\text{eff}} (\hat{a}_p \hat{b}^{\dagger 2} - \hat{a}_p^{\dagger} \hat{b}^2) - (\gamma_s + g_c^2 p) \hat{b}^{\dagger} \hat{b}, \quad (\text{C3c})$$

where $\partial_t = \partial/\partial t$. Applying the mean-field approximation, the instantaneous evolution of the average values of the operators is described as

$$\partial_t \langle \hat{a}_p \rangle = -iN g_{\text{eff}} \langle \hat{b}^2 \rangle - i\Omega^*/2 - (\kappa_p + J^2 p_\gamma) \langle \hat{a}_p \rangle / 2, \quad (\text{C4a})$$

$$\partial_t \langle \hat{b}^2 \rangle = -2iN g_{\text{eff}} \langle \hat{a}_p \rangle (2\langle \hat{b}^{\dagger} \hat{b} \rangle + 1) - (\gamma_s + g_c^2 p_\gamma + 2\gamma_c) \langle \hat{b}^2 \rangle, \quad (\text{C4b})$$

$$\partial_t \langle \hat{b}^{\dagger} \hat{b} \rangle = -4iN g_{\text{eff}} \text{Im}(\langle \hat{a}_p \rangle \langle \hat{b}^{\dagger 2} \rangle) - (\gamma_s + g_c^2 p) \langle \hat{b}^{\dagger} \hat{b} \rangle. \quad (\text{C4c})$$

Then, the time evolutions of $\langle \hat{b}^2 \rangle$ and $\langle \hat{b}^{\dagger} \hat{b} \rangle$ can be obtained by solving the coupled equations in Eq. (C4). After substituting $\langle \hat{b}^2 \rangle$ and $\langle \hat{b}^{\dagger} \hat{b} \rangle$ into Eq. (C2), the evolution of the spin squeezing parameter $\xi_{\mathcal{R}}^2$ is also obtained and then the minimum of the spin squeezing parameter $\xi_{\mathcal{R},\text{min}}^2$ can be achieved accordingly.

-
- [1] J. Ma, X.-G. Wang, C.-P. Sun, and F. Nori, Quantum spin squeezing, *Phys. Rep.* **509**, 89 (2011).
- [2] L. Pezzè, A. Smerzi, M. K. Oberthaler, R. Schmied, and P. Treutlein, Quantum metrology with nonclassical states of atomic ensembles, *Rev. Mod. Phys.* **90**, 035005 (2018).
- [3] M. A. Perlin, C.-L. Qu, and A. M. Rey, Spin squeezing with short-range spin-exchange interactions, *Phys. Rev. Lett.* **125**, 223401 (2020).
- [4] S.-Y. Bai and J.-H. An, Generating stable spin squeezing by squeezed-reservoir engineering, *Phys. Rev. Lett.* **127**, 083602 (2021).
- [5] D. J. Wineland, J. J. Bollinger, W. M. Itano, F. L. Moore, and D. J. Heinzen, Spin squeezing and reduced quantum noise in spectroscopy, *Phys. Rev. A* **46**, R6797 (1992).
- [6] D. J. Wineland, J. J. Bollinger, W. M. Itano, and D. J. Heinzen, Squeezed atomic states and projection noise in spectroscopy, *Phys. Rev. A* **50**, 67 (1994).
- [7] D. Ulam-Orgikh and M. Kitagawa, Spin squeezing and decoherence limit in ramsey spectroscopy, *Phys. Rev. A* **64**, 052106 (2001).
- [8] D. Döring, G. McDonald, J. E. Debs, C. Figl, P. A. Altin, H.-A. Bachor, N. P. Robins, and J. D. Close, Quantum-projection-noise-limited interferometry with coherent atoms in a ramsey-type setup, *Phys. Rev. A* **81**, 043633 (2010).
- [9] I. Kruse, K. Lange, J. Peise, B. Lücke, L. Pezzè, J. Arlt, W. Ertmer, C. Lisdat, L. Santos, A. Smerzi, and C. Klempt, Improvement of an atomic clock using squeezed vacuum, *Phys. Rev. Lett.* **117**, 143004 (2016).
- [10] E. S. Polzik, The squeeze goes on, *Nature* **453**, 45 (2008).
- [11] I. D. Leroux, M. H. Schleier-Smith, and V. Vuletić, Orientation-dependent entanglement lifetime in a squeezed atomic clock, *Phys. Rev. Lett.* **104**, 250801 (2010).
- [12] K. Goda, O. Miyakawa, E. E. Mikhailov, S. Saraf, R. Adhikari, K. McKenzie, R. Ward, S. Vass, A. J. Weinstein, and N. Mavalvala, A quantum-enhanced prototype gravitational-wave detector, *Nat. Phys.* **4**, 472 (2008).
- [13] D. Walls and P. Zoller, Enhanced sensitivity of a gravitational wave detector, *Phys. Lett. A* **85**, 118 (1981).
- [14] T. Bilitewski, L. De Marco, J.-R. Li, K. Matsuda, W. G. Tobias, G. Valtolina, J. Ye, and A. M. Rey, Dynamical generation of spin squeezing in ultracold dipolar molecules, *Phys. Rev. Lett.* **126**, 113401 (2021).
- [15] M. Bhattacharya, Spin squeezing a cold molecule, *Phys. Rev. A* **92**, 063823 (2015).
- [16] J. Estève, C. Gross, A. Weller, S. Giovanazzi, and M. K. Oberthaler, Squeezing and entanglement in a bose-einstein condensate, *Nature* **455**, 1216 (2008).
- [17] M. Fadel, T. Zibold, B. Décamps, and P. Treutlein, Spatial entanglement patterns and einstein-podolsky-rosen steering in bose-einstein condensates, *Science* **360**, 409 (2018).
- [18] X.-Y. Luo, Y.-Q. Zou, L.-N. Wu, Q. Liu, M.-F. Han, M. K. Tey, and L. You, Deterministic entanglement generation from driving through quantum phase transitions, *Science* **355**, 620 (2017).
- [19] L. Chen, Y.-B. Zhang, and H. Pu, Spin squeezing in a spin-orbit-coupled bose-einstein condensate, *Phys. Rev. A* **102**, 023317 (2020).
- [20] A. Kuzmich, K. Mølmer, and E. S. Polzik, Spin squeezing in an ensemble of atoms illuminated with squeezed light, *Phys. Rev. Lett.* **79**, 4782 (1997).
- [21] J. Hald, J. L. Sørensen, C. Schori, and E. S. Polzik, Spin squeezed atoms: A macroscopic entangled ensemble created by light, *Phys. Rev. Lett.* **83**, 1319 (1999).
- [22] B. Julsgaard, A. Kozhekin, and E. S. Polzik, Experimental long-lived entanglement of two macroscopic objects, *Nature* **413**, 400 (2001).
- [23] A. Kuzmich, L. Mandel, and N. P. Bigelow, Generation of spin squeezing via continuous quantum nondemolition measurement, *Phys. Rev. Lett.* **85**, 1594 (2000).
- [24] M. Koschorreck, M. Napolitano, B. Dubost, and M. W. Mitchell, Quantum nondemolition measurement of large-spin ensembles by dynamical decoupling, *Phys. Rev. Lett.* **105**, 093602 (2010).
- [25] T. Chalopin, C. Bouazza, A. Evrard, V. Makhhalov, D. Dreon, J. Dalibard, L. A. Sidorenkov, and S. Nascimbene, Quantum-enhanced sensing using non-classical spin states of a highly magnetic atom, *Nat. Commun.* **9**, 4955 (2018).
- [26] A. Evrard, V. Makhhalov, T. Chalopin, L. A. Sidorenkov, J. Dalibard, R. Lopes, and S. Nascimbene, Enhanced magnetic sensitivity with non-gaussian quantum fluctuations, *Phys. Rev. Lett.* **122**, 173601 (2019).
- [27] V. Macrì, F. Nori, S. Savasta, and D. Zueco, Spin squeezing by one-photon-two-atom excitation processes in atomic ensembles, *Phys. Rev. A* **101**, 053818 (2020).
- [28] K. Tucker, D. Barberena, R. J. Lewis-Swan, J. K. Thompson, J. G. Restrepo, and A. M. Rey, Facilitating spin squeezing generated by collective dynamics with single-particle decoherence, *Phys. Rev. A* **102**, 051701 (2020).
- [29] W. Qin, Y.-H. Chen, X. Wang, A. Miranowicz, and F. Nori, Strong spin squeezing induced by weak squeezing of light inside a cavity, *Nanophotonics (Berlin)* **9**, 4853 (2020).
- [30] K. Helmerson and L. You, Creating massive entanglement of bose-einstein condensed atoms, *Phys. Rev. Lett.* **87**, 170402 (2001).
- [31] Y.-C. Liu, Z.-F. Xu, G.-R. Jin, and L. You, Spin squeezing: Transforming one-axis twisting into two-axis twisting, *Phys. Rev. Lett.* **107**, 013601 (2011).
- [32] P. Groszkowski, H.-K. Lau, C. Leroux, L. C. G. Govia, and A. A. Clerk, Heisenberg-limited spin squeezing via bosonic parametric driving, *Phys. Rev. Lett.* **125**, 203601 (2020).
- [33] Y.-C. Zhang, X.-F. Zhou, X.-X. Zhou, G.-C. Guo, and Z.-W. Zhou, Cavity-assisted single-mode and two-mode spin-squeezed states via phase-locked atom-photon coupling, *Phys. Rev. Lett.* **118**, 083604 (2017).
- [34] W. Qin, A. Miranowicz, and F. Nori, Beating the 3 db limit for intracavity squeezing and its application to nondemolition qubit readout, *Phys. Rev. Lett.* **129**, 123602 (2022).
- [35] Z. Leghtas, S. Touzard, I. M. Pop, A. Kou, B. Vlastakis, A. Petrenko, K. M. Sliwa, A. Narla, S. Shankar, M. J. Hatridge, M. Reagor, L. Frunzio, R. J. Schoelkopf, M. Mirrahimi, and M. H. Devoret, Confining the state of light to a quantum manifold by engineered two-photon loss, *Science* **347**, 853 (2015).

- [36] C. W. S. Chang, C. Sabín, P. Forn-Díaz, F. Quijandría, A. M. Vadiraj, I. Nsanzineza, G. Johansson, and C. M. Wilson, Observation of three-photon spontaneous parametric down-conversion in a superconducting parametric cavity, *Phys. Rev. X* **10**, 011011 (2020).
- [37] R. Lescanne, M. Villiers, T. Peronin, A. Sarlette, M. Delbecq, B. Huard, T. Kontos, M. Mirrahimi, and Z. Leghtas, Exponential suppression of bit-flips in a qubit encoded in an oscillator, *Nat. Phys.* **16**, 509 (2020).
- [38] A. Vrajitoarea, Z.-W. Huang, P. Groszkowski, J. Koch, and A. A. Houck, Quantum control of an oscillator using a stimulated josephson nonlinearity, *Nat. Phys.* **16**, 211 (2019).
- [39] H. Hattermann, D. Bothner, L. Y. Ley, B. Ferdinand, D. Wiedmaier, L. Sárkány, R. Kleiner, D. Koelle, and J. Fortágh, Coupling ultracold atoms to a superconducting coplanar waveguide resonator, *Nat. Commun.* **8**, 2254 (2017).
- [40] J. Verdú, H. Zoubi, C. Koller, J. Majer, H. Ritsch, and J. Schmiedmayer, Strong magnetic coupling of an ultracold gas to a superconducting waveguide cavity, *Phys. Rev. Lett.* **103**, 043603 (2009).
- [41] M. Kaiser, C. Glaser, L. Y. Ley, J. Grimm, H. Hattermann, D. Bothner, D. Koelle, R. Kleiner, D. Petrosyan, A. Günther, and J. Fortágh, Cavity-driven rabi oscillations between rydberg states of atoms trapped on a superconducting atom chip, *Phys. Rev. Research* **4**, 013207 (2022).
- [42] J. G. Kroll, F. Borsoi, K. L. van der Enden, W. Uilhoorn, D. de Jong, M. Quintero-Pérez, D. J. van Woerkom, A. Bruno, S. R. Plissard, D. Car, E. Bakkers, M. C. Cassidy, and L. P. Kouwenhoven, Magnetic-field-resilient superconducting coplanar-waveguide resonators for hybrid circuit quantum electrodynamics experiments, *Phys. Rev. Applied* **11**, 064053 (2019).
- [43] S. Bernon, H. Hattermann, D. Bothner, M. Knufin, P. Weiss, F. Jessen, D. Cano, M. Kemmler, R. Kleiner, D. Koelle, and J. Fortágh, Manipulation and coherence of ultra-cold atoms on a superconducting atom chip, *Nat. Commun.* **4**, 2380 (2013).
- [44] A. Bruno, G. de Lange, S. Asaad, K. L. van der Enden, N. K. Langford, and L. DiCarlo, Reducing intrinsic loss in superconducting resonators by surface treatment and deep etching of silicon substrates, *Appl. Phys. Lett.* **106**, 182601 (2015).
- [45] M. Mirhosseini, E. Kim, V. S. Ferreira, M. Kalae, A. Sipahigil, A. J. Keller, and O. Painter, Superconducting metamaterials for waveguide quantum electrodynamics, *Nat. Commun.* **9**, 3706 (2018).
- [46] A. Blais, A. L. Grimsmo, S. M. Girvin, and A. Wallraff, Circuit quantum electrodynamics, *Rev. Mod. Phys.* **93**, 025005 (2021).
- [47] W. Qin, A. Miranowicz, H. Jing, and F. Nori, Generating long-lived macroscopically distinct superposition states in atomic ensembles, *Phys. Rev. Lett.* **127**, 093602 (2021).
- [48] Z. Ficek and S. Swain, *Quantum Interference and Coherence* (Springer New York, NY, USA, 2005).
- [49] D. Ran, W.-J. Shan, Z.-C. Shi, Z.-B. Yang, J. Song, and Y. Xia, Generation of nonclassical states in nonlinear oscillators via lyapunov control, *Phys. Rev. A* **102**, 022603 (2020).
- [50] S. Liu, D. Ran, Y.-H. Kang, Z.-C. Shi, J. Song, and Y. Xia, Accelerated and robust generation of w state by parametric amplification and inverse hamiltonian engineering, *Ann. Phys. (Berlin)* **532**, 2000002 (2020).
- [51] Y.-H. Kang, J. Song, and Y. Xia, Error-resistant nonadiabatic binomial-code geometric quantum computation using reverse engineering, *Opt. Lett.* **47**, 4099 (2022).
- [52] Y. Wang, C. Li, E. M. Sampuli, J. Song, Y. Jiang, and Y. Xia, Enhancement of coherent dipole coupling between two atoms via squeezing a cavity mode, *Phys. Rev. A* **99**, 023833 (2019).
- [53] Y. Wang, J.-L. Wu, J. Song, Y.-Y. Jiang, Z.-J. Zhang, and Y. Xia, Squeezing-enhanced atom-cavity interaction in coupled cavities with high dissipation rates, *Ann. Phys. (Berlin)* **531**, 1900220 (2019).
- [54] D.-L. Chen, Y.-H. Chen, Y. Liu, Z.-C. Shi, J. Song, and Y. Xia, Detecting a single atom in a cavity using the $\chi^{(2)}$ nonlinear medium, *Front. Phys. (Beijing)* **17**, 52501 (2022).
- [55] Y.-H. Chen, W. Qin, X. Wang, A. Miranowicz, and F. Nori, Shortcuts to adiabaticity for the quantum rabi model: Efficient generation of giant entangled cat states via parametric amplification, *Phys. Rev. Lett.* **126**, 023602 (2021).
- [56] W. Qin, V. Macrì, A. Miranowicz, S. Savasta, and F. Nori, Emission of photon pairs by mechanical stimulation of the squeezed vacuum, *Phys. Rev. A* **100**, 062501 (2019).
- [57] D. F. James and J. Jerke, Effective hamiltonian theory and its applications in quantum information, *Can. J. Phys.* **85**, 625 (2007).
- [58] W.-J. Shao, C.-F. Wu, and X.-L. Feng, Generalized james' effective hamiltonian method, *Phys. Rev. A* **95**, 032124 (2017).
- [59] L. A. Williamson, Y.-H. Chen, and J. J. Longdell, Magneto-optic modulator with unit quantum efficiency, *Phys. Rev. Lett.* **113**, 203601 (2014).
- [60] N. Lauk, N. Sinclair, S. Barzanjeh, J. P. Covey, M. Saffman, M. Spiropulu, and C. Simon, Perspectives on quantum transduction, *Quantum Science and Technology* **5**, 020501 (2020).
- [61] T. Liu, J.-L. Zhao, B.-Q. Guo, Q.-C. Wu, Y.-H. Zhou, and C.-P. Yang, One-step implementation of a coherent conversion between microwave and optical cavities via an ensemble of nitrogen-vacancy centers, *Phys. Rev. A* **103**, 023706 (2021).
- [62] N. Shammah, S. Ahmed, N. Lambert, S. De Liberato, and F. Nori, Open quantum systems with local and collective incoherent processes: Efficient numerical simulations using permutational invariance, *Phys. Rev. A* **98**, 063815 (2018).
- [63] J. Gelhausen, M. Buchhold, and P. Strack, Many-body quantum optics with decaying atomic spin states: (γ, κ) dicke model, *Phys. Rev. A* **95**, 063824 (2017).
- [64] J. Dalibard, Y. Castin, and K. Mølmer, Wave-function approach to dissipative processes in quantum optics, *Phys. Rev. Lett.* **68**, 580 (1992).
- [65] F. Reiter and A. S. Sørensen, Effective operator formalism for open quantum systems, *Phys. Rev. A* **85**, 032111 (2012).
- [66] Y.-H. Chen, Z.-C. Shi, J. Song, Y. Xia, and S.-B. Zheng, Accelerated and noise-resistant generation of high-fidelity steady-state entanglement with rydberg atoms, *Phys. Rev. A* **97**, 032328 (2018).
- [67] R. Amsüss, C. Koller, T. Nöbauer, S. Putz, S. Rotter, K. Sandner, S. Schneider, M. Schramböck, G. Stein-

- hauser, H. Ritsch, J. Schmiedmayer, and J. Majer, Cavity qed with magnetically coupled collective spin states, *Phys. Rev. Lett.* **107**, 060502 (2011).
- [68] Y. Kubo, F. R. Ong, P. Bertet, D. Vion, V. Jacques, D. Zheng, A. Dréau, J.-F. Roch, A. Auffeves, F. Jelezko, J. Wrachtrup, M. F. Barthe, P. Bergonzo, and D. Esteve, Strong coupling of a spin ensemble to a superconducting resonator, *Phys. Rev. Lett.* **105**, 140502 (2010).
- [69] Y. Kubo, I. Diniz, A. Dewes, V. Jacques, A. Dréau, J.-F. Roch, A. Auffeves, D. Vion, D. Esteve, and P. Bertet, Storage and retrieval of a microwave field in a spin ensemble, *Phys. Rev. A* **85**, 012333 (2012).
- [70] T. Astner, S. Nevlacsil, N. Peterschofsky, A. Angerer, S. Rotter, S. Putz, J. Schmiedmayer, and J. Majer, Coherent coupling of remote spin ensembles via a cavity bus, *Phys. Rev. Lett.* **118**, 140502 (2017).
- [71] S. Putz, D. O. Krimer, R. Amsüss, A. Valookaran, T. Nöbauer, J. Schmiedmayer, S. Rotter, and J. Majer, Protecting a spin ensemble against decoherence in the strong-coupling regime of cavity QED, *Nat. Phys.* **10**, 720 (2014).
- [72] P. L. Stanwix, L. M. Pham, J. R. Maze, D. Le Sage, T. K. Yeung, P. Cappellaro, P. R. Hemmer, A. Yacoby, M. D. Lukin, and R. L. Walsworth, Coherence of nitrogen-vacancy electronic spin ensembles in diamond, *Phys. Rev. B* **82**, 201201 (2010).
- [73] L.-Y. Cheng, H.-F. Wang, S. Zhang, and K.-H. Yeon, Quantum state engineering with nitrogen-vacancy centers coupled to low-q microresonator, *Opt. Express* **21**, 5988 (2013).
- [74] X. Han, Q. Guo, A.-D. Zhu, S. Zhang, and H.-F. Wang, Effective w-state fusion strategies in nitrogen-vacancy centers via coupling to microtoroidal resonators, *Opt. Express* **25**, 17701 (2017).
- [75] Z. Jin, S. L. Su, and S. Zhang, Preparation of a steady entangled state of two nitrogen-vacancy centers by simultaneously utilizing two dissipative factors, *Phys. Rev. A* **100**, 052332 (2019).
- [76] L.-Y. Cheng, Q. Guo, H.-F. Wang, and S. Zhang, Direct entanglement measurement of werner state with cavity-assisted spin-photon interaction system, *Quantum Information Processing* **18**, 214 (2019).
- [77] L.-Y. Cheng, G.-H. Yang, Q. Guo, H.-F. Wang, and S. Zhang, Direct measurement of nonlocal entanglement of two-qubit spin quantum states, *Scientific Reports* **6**, 19482 (2016).
- [78] T. Holstein and H. Primakoff, Field dependence of the intrinsic domain magnetization of a ferromagnet, *Phys. Rev.* **58**, 1098 (1940).